

A high-accuracy, small field of view star guider with application to SNAP

Aurélia Secroun[†] and Michael Lampton
Space Sciences Laboratory, U.C. Berkeley

Michael Levi
Lawrence Berkeley National Laboratory, U.C. Berkeley

October 18, 2000

Abstract. To accomplish its mission, the spaceborne observatory SNAP (SuperNova Acceleration Probe) requires a pointing stability of < 0.03 arcseconds during exposures lasting up to 500 seconds. A Monte Carlo simulation of the photoelectron statistics from the guiding star investigates geometrical (such as the pixel size of the detector or the plate scale) and physical parameters (such as the magnitude of the star). It is shown that simple centroiding calculations can lead to the desired accuracy with guide stars as faint as magnitude 16. Availability of these stars is verified thanks to the HST Guide Star Catalog complemented with a statistical model of the distribution of stars. Thus a through-the-lens sensor that uses stars as faint as magnitude 16 to provide the necessary guiding signals is feasible.

Keywords: star guider, star tracker, centroid

1. Introduction

In one year of study, the SNAP (SuperNova Acceleration Probe) satellite can discover, follow the light curve, and obtain spectra at peak brightness for more than 2000 supernovae. SNAP instrumentation includes a wide field optical imager (field of view of one square degree) and a small IR imager, which, combined with filters, will allow photometry from 0.35 to $1.7 \mu\text{m}$ and a three arm spectrograph sensitive in the same range of wavelengths. SNAP instrumentation will be used with a simple, predetermined observing strategy designed to monitor a 20 square degree region of sky both near the north ecliptic pole ($16 \text{ h } 25 \text{ min } + 57 \text{ deg}$) and near the south ecliptic pole ($4 \text{ h } 30 \text{ min } - 52 \text{ deg}$), discovering and following supernovae that explode in these regions. More information on the scientific background of this mission can be found at the URL <http://snap.lbl.gov>.

The data from the wide field optical imager will serve both as search images and for follow-up photometry. The detection of supernovae is accomplished by a repeated comparison of fixed fields to reference images. The optical photometer obtains wide-field frames overlapping the positions of

[†] Now at Laboratoire de Physique Nucléaire et Hautes Énergies, Paris



the discovery frames. The IR photometer obtains small frames determined by pointing the satellite at the previously discovered supernova. Thus the follow-up optical photometry is obtained without specific knowledge of the location of new supernovae, whereas the follow-up IR photometry will require specific knowledge of the location of each new supernova. Similarly, spectroscopy will require pointing specifically at the newly discovered supernova. Moreover, the typical 500 second exposures of SNAP will require guiding stability better than 0.03 arcseconds to achieve photometric errors below one percent.

Consequently, SNAP's ACS (Attitude Control System) system must fulfill two functions: pointing the whole spacecraft to a given direction (namely to a supernova that is to be studied) and keeping the focal plane of each instrument stable during the whole acquisition time. A coarse pointing accuracy of approximately 2 arcseconds can be easily achieved on a spacecraft with a suitably rigid structure by gyroscopes and other standard instruments. Nevertheless, the coarse guider will have to be augmented by a higher accuracy tracking system to achieve the required fine accuracy of 0.03 arcseconds.

Star trackers are commonly used for fine guiding. Many different techniques exist, for which three aspects should be distinguished: first, the kind of object that will be observed for guiding, then the type of device used to acquire data and finally the algorithm applied to the data acquired. The target may be either a set of stars, for which the relative position is measured, or a wide-angle field of stars (Jorgensen and Pickles, 1998), for which the image is correlated against a star catalogue in memory, or a single star, for which, for instance, the center is measured. The cases of a set of stars or a wide-angle field of stars both require a large field of view which we cannot afford since as much as possible must be reserved to the wide field imager in order to fulfill the scientific goals.

In order to correct for all three pitch, yaw and roll, two stars are necessary. When our guider is part of the image field, the errors in pitch and yaw directly give errors in X and Y. However the third axis, roll, is around the field, causing circulation of stars, and because our field is much less than one radian, the position errors from roll are much less important (about 100 times less important). Commercial attitude control sensors use two or more simple star cameras and will give us three axis information good to about an arc second in all three axes. So our fine guidance does not need to measure roll, just X and Y. Of course, if we guide on several stars, we could estimate roll also ; but that would not be particularly accurate, nor is it important for our mission. Thus, in our case, roll will be corrected for by the coarse ACS system and thus our star guider will only need one reference star. In this paper we address the

issue of the achievable guiding errors resulting from sensor noise.

Of course the type of device used might make a difference. Let us consider today's technology:

- quadrant CCDs : used particularly for extended objects (Clampin et al., 1990);
- CCD cameras;
- active pixel matrices: still new and not as flight proven as the CCD cameras (Liebe et al., 1998; Yadid-Pecht et al., 1997).

The type of device we will use is still under discussion. However, whether a CCD camera or an active pixel matrix is chosen, guiding on a single star must follow two steps:

1. scan all the pixels in search of a good guiding star;
2. repeatedly determine the center of the guiding star image and deliver x and y error signals to the ACS for pointing correction.

Various algorithms (Chmielowski and Klein, 1993; Gwo, 1997; Salomon and Glavich, 1980) have been proposed to determine the position of a star, among which centroiding (Deng and Bergen, 1987) (which evaluates the center of the star blur) is certainly the most widespread. The aim is usually to offer a good compromise between the time used for the calculation (which is limited by the need for real time correction of the spacecraft pointing) and the precision obtained.

Hereafter, we want to show that it is possible, using star light gathered by the full two meter telescope aperture of SNAP, to guide with a single star and centroiding calculations to the desired accuracy of 0.03 arcseconds in a single 30 ms sample over 95 % of the planned SNAP survey regions. Further enhancement of the resolution can certainly be obtained by co-adding, by a Kalman filter or through image position interpolation algorithms and lead to an even better accuracy. The present work includes a simulation of the noisy star as it would be recorded by a pixellized detector, as well as a simulation of the supernova pointing. These simulations will allow us to define the characteristics of our star tracker necessary for the best results.

2. How bright a star do we need for guiding?

Taken that star guiding is to be obtained through the observation of a single star, the question can be restated as: what configuration will allow us to reach the desired guider RMS position error of 0.03 arcseconds? The configuration includes parameters such as the magnitude of the star, the noise level, the characteristics of the sensor, and the algorithm. It is important to note that the large aperture of the telescope (2.0 meters) allows us to work with faint stars, while the long focal length (20 meters) makes bright stars unlikely to be found.

2.1. IDEAL DETECTOR

The fundamental performance limit for guiding accuracy is set by the photon arrival statistics. To make this limit quantitative, consider an ideal noiseless 2-D photon sensor with 100 % quantum efficiency and perfect (unpixellized) image quality.

2.1.1. *Signal from the star*

The star blur is represented by a 2-dimensional Gaussian, whose integral is the total number of photons from the star as given below. The standard deviation of the Gaussian is a parameter that defines the size of the star blur. In all this study, we assume a star blur size of 0.1 arcseconds (or FWHM = 0.235 arcseconds),* as determined by diffraction. The total number of photons N_{ph} received on a detector from a star with visible magnitude m_V is given in equation 1.

$$N_{ph} = f_{\lambda} \cdot \Delta t \cdot A \cdot \Delta \lambda \cdot T \cdot \frac{1}{E_{ph}} \quad (1)$$

* The standard deviation σ is related to the full width at half maximum through $FWHM = \sigma \cdot 2\sqrt{2\log 2} \approx 2.35\sigma$

$$\text{where } \left\{ \begin{array}{l} f_{\lambda} \text{ is the spectral irradiance of the star calculated from its} \\ \text{visible magnitude } m_V \text{ through } f_{\lambda} = 10^{-0.4m_V - 8.44} \text{ (erg} \\ \text{cm}^{-2} \text{ s}^{-1} \text{ \AA}^{-1}) \\ \Delta t \text{ is the integration time (s)} \\ A \text{ is the aperture obtained from the diameter } d \text{ of the} \\ \text{primary mirror through } A = \frac{\pi d^2}{4} \text{ (cm}^2\text{)} \\ \Delta \lambda \text{ is the spectral range of observed photons (\AA)} \\ T \text{ is the total transmission of the system, which should} \\ \text{include the transmission of the optics and the quantum} \\ \text{efficiency of the detector} \\ E_{ph} \text{ is the central energy of the photons determined at a} \\ \text{given wavelength } \lambda_0 \text{ as } E_{ph} = \frac{hc}{\lambda_0} \text{ (erg).} \end{array} \right.$$

2.1.2. Guiding

Each photon is a sample from a population of events distributed as a 2-D Gaussian distribution with zero mean and standard deviation σ along each axis. The mathematical centroid of N independent events will have zero mean and RMS deviations along both axes given by equation 2.

$$X_{RMS} = Y_{RMS} = \frac{\sigma}{\sqrt{N}} \quad (2)$$

Quite generally then to achieve a specified 1-D centroid accuracy, we will have to provide a sufficient number of photons as defined by equation 3.

$$N_{min} = \left(\frac{\sigma}{X_{RMS}} \right)^2 \quad (3)$$

To meet the requirements of the SNAP mission, with $\sigma = 0.1$ arcseconds and $X_{RMS} = 0.03$ arcseconds, the minimum number of photons received on the sensor should be $N_{min} = 11$ photons. On a 2 meter telescope with a 60 % efficient optical train and an ideal detector with a 100 % efficiency, a bandwidth of $0.6 \mu\text{m}$ at V-band (say centered on 700 nm), and a 30 millisecond integration time, this photon accumulation requires a star of visible magnitude as bright as 20.

2.2. REAL DETECTOR

A more realistic detector has imperfect quantum efficiency, readout noise, and discrete pixellization. These factors complicate the centroid determination and require a brighter star on which to guide. We address these complications in the paragraphs that follow.

2.2.1. Monte Carlo simulation

A Monte Carlo simulation of the signal received on the sensor including the star blur (as defined in 2.1.1) and the noise can help us determine some characteristics of the guider as well as specific conditions in which it might need to be used. Statistics on the centroid call for a large number of trials, in which both the noise and the actual position of the star within the pixel must be randomized. Indeed the relative position of the star within a pixel affects the distribution of the photons between the neighboring pixels, and thus the effect of the noise on those pixels, and in the end the estimated value for the star center.

In particular, this simulation allows us to explore the following parameters:

- the linear size* of a pixel of the detector,
- the integration time,
- the magnitude of the guiding star in the V-band,
- the size of the star blur on the guider (or equivalently the plate scale on the guider),
- and the number of pixels used for the calculations.

In the simulation, the following values for the parameters, as defined in 2.1.1, are assumed:

- the telescope has an aperture of 2 meters,
- the wavelength range is a rectangular approximation of the silicon response in the V-band, with a central wavelength λ_0 of 700 nm and a spectral interval $\Delta\lambda$ of 600 nm,
- the overall throughput, including the transmission of the telescope and the quantum efficiency of the detector, is 25 %.

2.2.2. Noise model

There are essentially three components to the noise in each pixel, in order of importance:

1. the shot noise from the star photons,
2. the readout noise which may be some 30 electrons per pixel when integrating at rates within the video range,

* Note that the linear size (in μm) is the product of the angular size (in arcseconds) by the focal length of the telescope.

3. the background sky noise which becomes in fact a component of the shot noise and can be evaluated as equivalent to a star of magnitude 23 per square arcseconds as seen in figure 1 of (O'Connell, 1987). This value is defined for space observation in a direction typical of extragalactic pointings. At wavelengths longer than 3000 Å, it is dominated by zodiacal scattering of sunlight.

Other noises like dark current or responsivity for different pixels are expected to be negligible compared to shot noise and thus are not taken into consideration here.

Noise is modeled as a normal statistical distribution, with zero mean and standard deviation σ given in equation 4. The processes are independent and therefore their variances add.

$$\sigma^2 = N_{ph/px} + \sigma_{readout}^2 + N_{skyph} \quad (4)$$

$$\text{where } \left\{ \begin{array}{l} \sqrt{N_{ph/px}} \text{ is the shot noise from the star photons falling in} \\ \text{the given pixel} \\ \sigma_{readout} \text{ is the readout noise} \\ \sqrt{N_{skyph}} \text{ is the shot noise from the background sky falling} \\ \text{in the given pixel.} \end{array} \right.$$

2.2.3. Centroiding

The center of the star is determined by a simple centroiding calculation. Equations 5 and 6 give the two dimensional centroid that creates estimators of both x and y position coordinates.

$$\tilde{X} = \frac{\sum_i^n \sum_j^n i \cdot q_{i,j}}{\sum_i^n \sum_j^n q_{i,j}} \quad (5)$$

$$\tilde{Y} = \frac{\sum_i^n \sum_j^n j \cdot q_{i,j}}{\sum_i^n \sum_j^n q_{i,j}} \quad (6)$$

$$\text{where } * \left\{ \begin{array}{l} n \text{ is the number of pixels in one direction, and } n \cdot n \text{ the total} \\ \text{number of pixels over which the centroid is calculated} \\ i [j] \text{ is the number of the } i^{\text{th}} [j^{\text{th}}] \text{ pixel} \\ q_{i,j} \text{ is the charge of pixel } (i, j), \text{ which is the sum of the} \\ \text{signal from the star and the noise as defined in section} \\ 2.2.2. \end{array} \right.$$

2.3. RESULTS

The results presented here are obtained for a magnitude of the guiding star between 9 and 18, an integration time between 10 and 1000 ms (or in other words a frame rate between 1 and 100 frames per second), for typical read-out noises between 10 and 30 electrons, and an angular pixel size of 0.1 arcseconds.

2.3.1. *Star blur size and number of pixels used in the calculation*

Figure 1 shows the RMS noise error[†] obtained for four magnitudes of guiding star (9, 14, 15 and 16), a pixel size of 0.1 arcseconds, a typical integration time of 30 ms and a typical readout noise of 30 electrons. The RMS star blur size defined in equation 2 is varied between 0.5 and 5 pixels. The number of pixels is varied between 2 and 4.

For any magnitude of the guiding star and any number of pixels used for the calculation, the noise error as a function of the star blur size reaches a minimum. This minimum corresponds to a star blur size of 1.5 pixels when centroiding over 2 pixels, a size of about 2 pixels when centroiding over 3 pixels and a size of about 3 pixels when centroiding over 4 pixels. Indeed, when the star blur is smaller than a pixel, most of the photons fall into one single pixel and a lot of information gets lost so that no improvement is obtained in the error and even to an extreme one could expect that the error would degrade.

Since obviously one pixel cannot bring any information, a calculation over 2 pixels is the minimum number over which the calculation remains meaningful. Unlike what might be naturally expected, adding pixels into the calculation mostly increases the error and the conclusion is that we should use only 2 pixels for the calculations. In particular, one might expect that when the blur is not well centered for instance on a 2 x 2 pixel square, then we might gain information and thus precision by calculating the centroid over 3

* The calculations need not be applied to the whole detector area and on the contrary should be restricted to a few pixels in order to limit the destructive effect of noise.

† The RMS noise error is expressed in milliarcseconds, thus taking into account the plate scale defined as the ratio of the star blur size in μm on the guider to that in arcseconds viewed from the telescope.

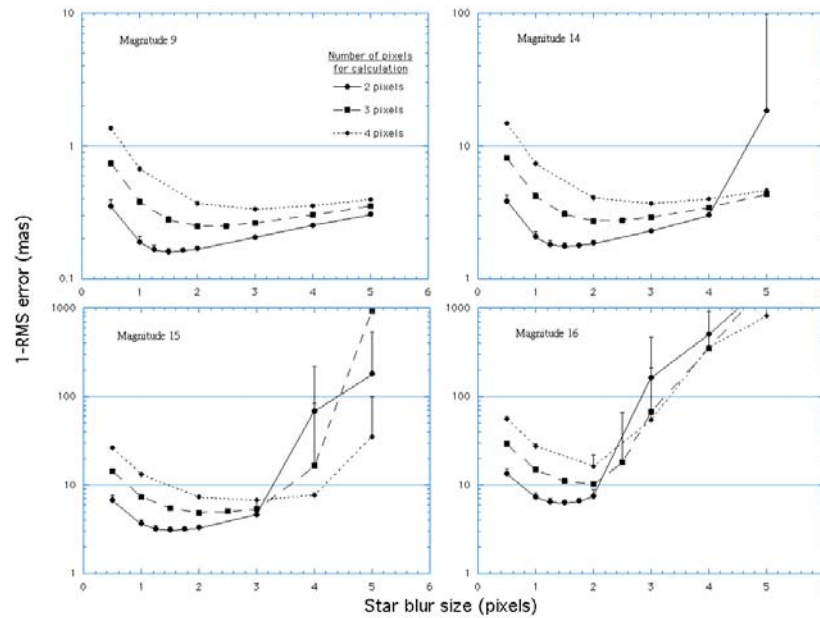


Figure 1. One-sigma width of distribution of x or y centroids, for various values of RMS star blur size. Integration time of 30 ms, angular pixel size of 0.1 arcseconds, readout noise of 30 electrons.

pixels. The graphs of figure 1 show clearly that this is not the case. Overall, the noise error is always the smallest when centroid calculations are applied on 2 pixels.

In conclusion, the minimum noise error is obtained for a star blur size of 1.5 pixels and calculations of the centroid over 2 pixels. We will use those figures in the following sections. Note also that a consequence of the 2 pixel figure is that none of the common filtering algorithms, such as curve fitting, is worth being applied. Two pixel centroiding is a computational task sufficiently simple to be accomplished entirely in hardware and can therefore easily sustain the real time frame rates needed for SNAP.

2.3.2. Systematic error

The centroid is a biased estimator, for which the bias is a function of the position of the star. Figure 2 shows the evaluated centroid as a function of the position of the star, with (dots) and without noise (solid line). This bias is mostly due to the discrete quality of the centroid estimator. If not corrected for, it will add an error that depends on the relative displacement of the guiding star. In fact, as figure 2 shows it, if most of the bias can be corrected for, a little error will still remain (represented by the random distance to the

noiseless bias). This error appears in the following graphs through the error bars.

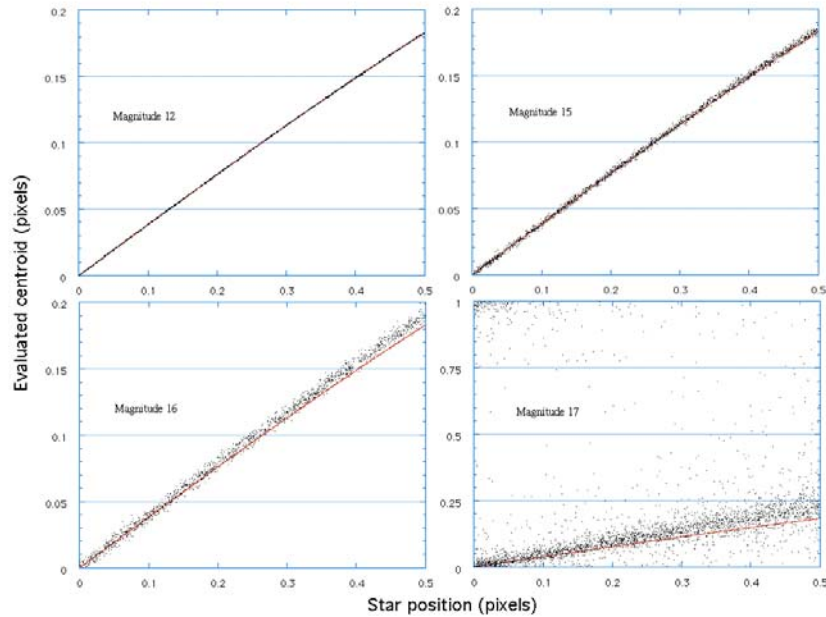


Figure 2. Systematic errors. The solid line shows the relation between star position and evaluated centroid in the absence of noise, and the black dots points in presence of noise. Integration time of 30 ms, angular pixel size of 0.1 arcseconds, readout noise of 30 electrons.

2.3.3. Noise error

Figure 3 shows the 1-RMS error due to the added noise (see section 2.2.2) obtained for different integration times and different magnitudes of guiding star. For an integration time of 30 ms, the statistical one-sigma centroid distribution width is less than 0.01 arcseconds for stars brighter than magnitude 16. For longer integration times (100 or 200 ms), stars of magnitude 17 or 18 reach the same low error of their statistical distribution.

2.3.4. Effect of the linear size of the pixel

Figure 4 shows the noise error obtained for different magnitudes of guiding star and specifically for a linear pixel size of 13 and 18 μm . The RMS error in arcseconds does not depend on the linear pixel size. This result comes as a direct consequence of our calculations. Indeed, the latter were made so that the star blur matched exactly one and a half pixel (whichever size the pixel might have). In other words, the plate scale was chosen accordingly. Consequently, this leaves a freedom in the technological choice for the linear

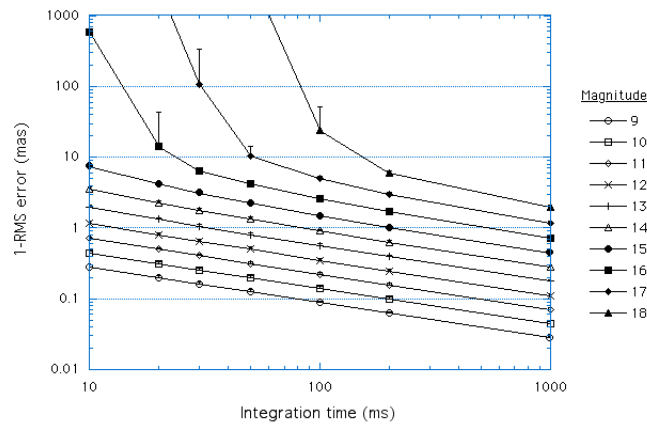


Figure 3. Noise error. Star blur of 1.5 pixels, readout noise of 30 electrons, angular pixel size of 0.1 arcseconds.

pixel size and a possible adjustment of the plate scale according to available pixel sizes.

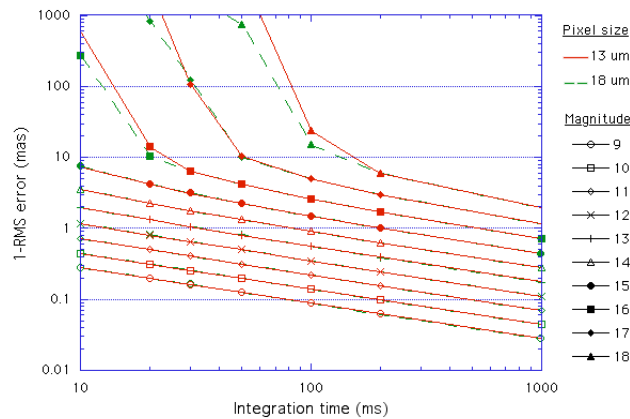


Figure 4. Effect of pixel size. Star blur of 1.5 pixels, readout noise of 30 electrons.

2.3.5. Effect of the readout noise

Figure 5 shows the noise error obtained for different magnitudes of guiding star and in particular for a readout noise of either 10 or 30 electrons. One may observe two zones, whether shot noise is dominating or not. In the case of dominating shot noise, that is to say as seen on the graph for magnitudes brighter than 15 and/or long enough integration times, the effect of readout noise is negligible and, the 1-RMS error is the same in either case. In general, however, the worst case guider performance occurs with the fainter stars, where readout noise dominates.

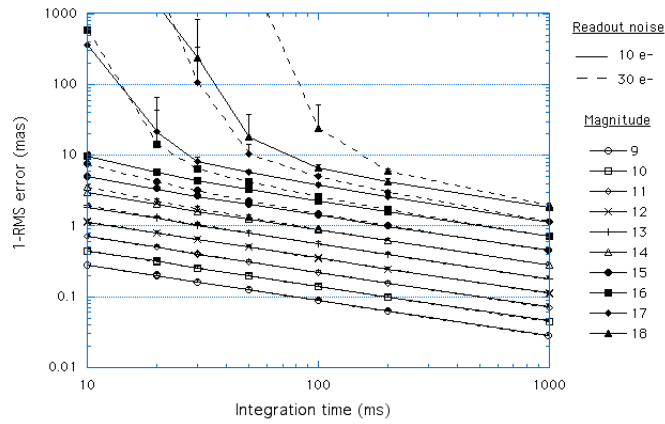


Figure 5. Effect of readout noise. Star blur of 1.5 pixels, angular pixel size of 0.1 arcseconds.

2.4. SUMMARY

The RMS error of our sensor's noise distribution will not interfere with the desired global pointing accuracy of 0.03 arcseconds, when the sensor is used at a 30 Hz rate and with a reference star of magnitude at most 16 (possibly 17, if either the rate is a bit slower or the readout noise is minimized). The linear pixel size has no effect on this conclusion. The star blur should be concentrated on 1.5 pixels with appropriate optics. The centroid should be calculated on a 2 x 2 pixel square. We would like to note that saturation may appear for guiding stars of magnitude less than 9. But this is a very rare case, less than 3 % of the time and thus it should be no problem to find another star for guiding.

3. Can we point at any supernova in the field of view?

We just showed that we need a 16 magnitude star for our fast guiding. But what fraction of randomly chosen star fields will contain a star this bright? This could be restated as: how big should the detector area be to assure the presence of a 16 magnitude star in its field of view 95 % of the time? We address this question in two ways: first, using a statistical model of star magnitudes, and secondly, using actual star fields from our SNAP survey regions.

3.1. STATISTICAL MODEL FOR THE DISTRIBUTION OF STARS

C.W. Allen (Allen, 1973) gives the average number of stars for different magnitudes and different galactic latitudes. Figure 6 shows those values as a function of the visible magnitude of the star.

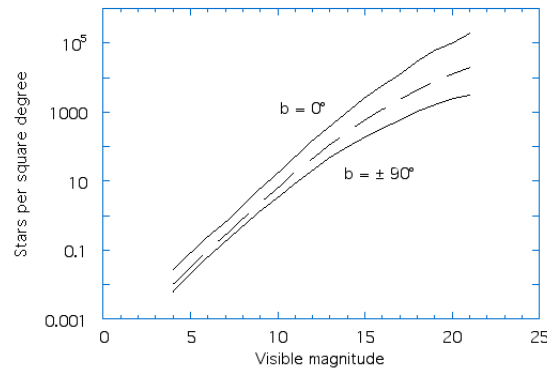


Figure 6. Mean star densities. b denotes the galactic latitude.

The Poisson law describes the probabilities of observing various numbers of independent events given their mean rate of occurrence. According to the Poisson law, the probability of getting at least one star in a given field of view is:

$$P(k \geq 1) = 1 - \exp(-m) \quad (7)$$

where $\begin{cases} k \text{ is the number of stars in the field of view} \\ m \text{ is the average number of stars.} \end{cases}$

3.2. GUIDE STAR CATALOG

The Poisson law expresses the statistics of independent events, and cannot be expected to describe actual star clustering. We therefore extended our study to include actual star counts in the SNAP survey regions. The Guide Star Catalog contains photometric and positional information about stars of magnitude up to 16 all over the sky gathered for the Hubble Space Telescope. It is available on the Internet.* We selected one area near the north ecliptic pole and another near the south ecliptic pole. Each area represents a square of size 5 x 5 degrees around the point of coordinates 16 h 25 min + 57 deg near the north ecliptic pole and the point of coordinates 4 h 30 min - 52 deg near the south ecliptic pole. The north area contains 11465 stars of magnitude up to 15.5 and the south area contains 12467 stars of magnitude up to 16.2, with the distribution shown on figure 7. The spatial distribution of stars are shown in figure 8 (a) and (b). It seems relatively uniform except for some areas which appear more dense, maybe due to different conditions of acquisition of these.

* <http://www-gsss.stsci.edu/gsc/gsc.html>

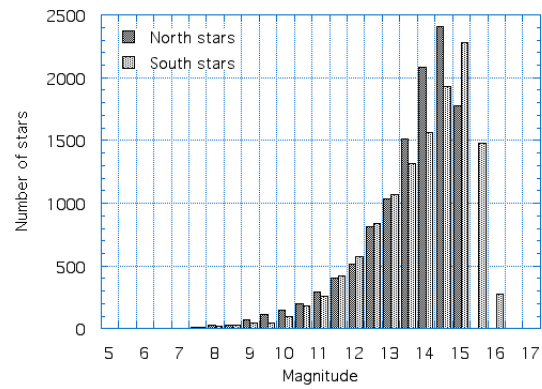
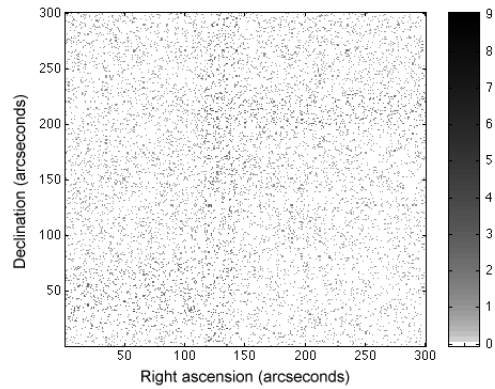
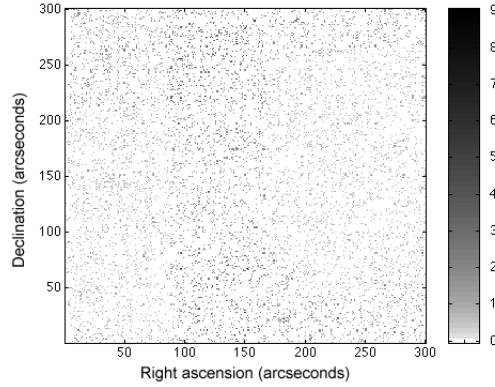


Figure 7. Histogram of the stars in the Guide Star Catalog.



(a)



(b)

Figure 8. Spatial distribution of stars at the north (a) and south ecliptic pole (b). Each dot represents the number of stars in a square arcminute with a gray level following the scale on the side of the map. Right ascension and declination are relative to the poles coordinates and represent a square of 5 x 5 degrees.

3.3. RESULTS

On the basis of the Guide Star Catalog information, a Monte Carlo code simulates the search of a possible guiding star within a given field of view (namely the size of the guider), when the whole spacecraft is pointing to a defined direction corresponding to the supernova under study. It stops as soon as one star is found.

There are essentially two parameters: the limit magnitude of the guiding star (varied between 9 and 16), and the size of the search field of view. We have chosen four different sizes:

- 100 x 100 arcseconds square,
- 100 x 200 arcseconds square,
- 200 x 200 arcseconds square,
- and 360 x 360 arcseconds square.

This allows to optimize the field of view of our guider required for reaching the desired pointing accuracy, in relation with the results obtained in section 2. The question we want to answer is: how big should the guider's field of view be to contain a star of magnitude 16 with a confidence of at least 95 %?

3.3.1. *Real stars*

Figure 9 shows the results from the Monte Carlo simulation both at the north and south ecliptic poles for 4 sizes of the field of view, as introduced above. We can observe that, in either case, we will definitely need a field of view of at least 200 x 200 arcseconds square.

3.3.2. *Comparison of statistical model with real star distribution*

Figure 10 is a graph equivalent to that of figure 9 derived from the statistical model, for the purpose of extrapolating the data to fainter magnitudes. In these calculations, the distribution of the stars is supposed to be uniform over the area of interest and the number of stars is derived from the model described in section 3.1 for a galactic latitude of 30 degrees. The model leads to the same conclusion that for a guiding star of magnitude 16, we will need at least a field of 200 x 200 arcseconds square. We also learn that, if for instance we can tolerate slower frame rates, guiding on a star of magnitude 17 only requires only a smaller area of 100 x 200 arcseconds square.

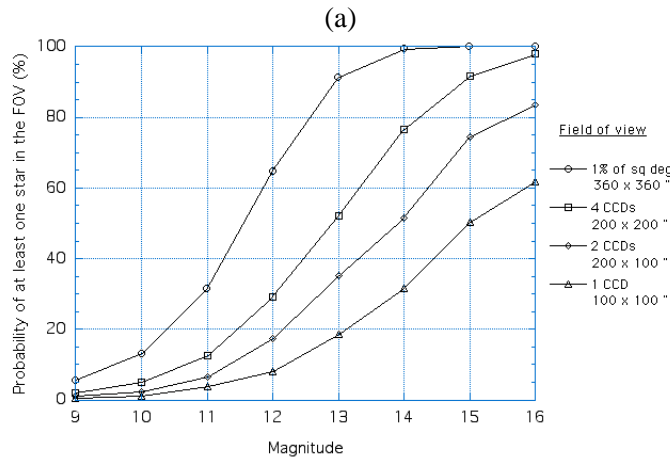
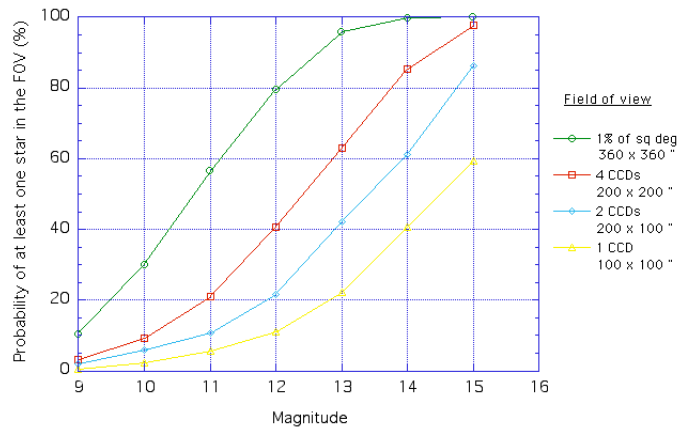


Figure 9. Presence of stars at the north (a) and south (b) ecliptic pole. The dots represent the number of guide stars per square arcminute.

4. Conclusion

Using a Monte Carlo simulation of the guide star signal and noise, and the distribution of stars in the real sky, we have shown that we will be able to sense at least 95 % of the observed sky with 0.03 arcseconds RMS accuracy, at a 30 Hz frame rate and with a detector area of 200 x 200 arcseconds. For the SNAP mission, we recommend the use of at least four 1024 x 1024 pixel CCD cameras, whose current technological characteristics correspond to the desired ones.

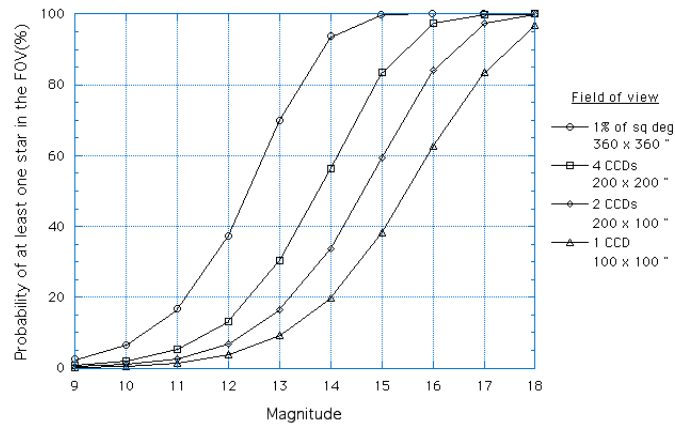


Figure 10. Presence of stars as derived from the statistical model.

References

- Allen, C.: 1973, *Astrophysical Quantities*. The Athlone Press.
- Chmielowski, M. and L. Klein: 1993, 'A High-Precision, Real-Time Position-Locating Algorithm for CCD-based Sun and Star Trackers'. *Publications of the Astronomical Society of the Pacific* **105**, 114–116.
- Clampin, M., S. Durrance, R. Barkhouser, et al.: 1990, 'A Quadrant-CCD star tracker'. In: *SPIE Charge-Coupled Devices and Solid State Optical Sensors*, Vol. 1242. pp. 217–222.
- Deng, T.-C. and T. L. Bergen: 1987, 'Accuracy of Position Estimation by Centroid'. In: *SPIE Intelligent Robots and Computer Vision: Sixth in a Series*, Vol. 848. pp. 141–150.
- Gwo, D.-H.: 1997, 'Robust guide-star algorithm proposed for Gravity Probe-B relativity mission'. In: *SPIE Telescope Control Systems II*, Vol. 3112. pp. 320–327.
- Jorgensen, J. and A. Pickles: 1998, 'Fast and robust pointing and tracking using a second-generation star tracker'. In: *SPIE Telescope Control Systems III*, Vol. 3351. pp. 51–61.
- Liebe, C., E. Dennison, B. Hancock, et al.: 1998, 'Active pixel sensor based star tracker'. In: *IEEE Aerospace Conference Proceedings*, Vol. 1. pp. 119–127.
- O'Connell, R. W.: 1987, 'Ultraviolet Detection of Very Low-Surface-Brightness Objects'. *The Astronomical Journal* **94**(4), 876–882.
- Salomon, P. M. and T. A. Glavich: 1980, 'Image signal processing in sub-pixel accuracy star trackers'. In: *SPIE Smart Sensors II*, Vol. 252. pp. 64–74.
- Yadid-Pecht, O., B. Pain, C. Staller, et al.: 1997, 'CMOS active pixel sensor star tracker with regional electronic shutter'. *IEEE Journal of Solid-State Circuits* **32**, 285–288.

